A multi-objective predictive control strategy for enhancing primary frequency support with wind farms

S. Siniscalchi-Minna[1,3], M. De Prada[1], F. D. Bianchi[2], C. Ocampo-Martinez[3] and B. De Schutter[4]

[1]Catalonia Institute for Energy Research, IREC, Jardins de le Dones de Negre, s/n Barcelona, Spain.
[2]CONICET and Instituto Balseiro, Bustillos 9500, S.C. Bariloche, Argentina.
[3]Automatic Control Department, Universitat Politècnica de Catalunya, Institut de Ròbotica i Informàtica Industrial (CSIC-UPC), Llorens i Artigas, 4-6, 08028 Barcelona, Spain.
[4] Delft Center for Systems and Control, Delft University of Technology, The Netherlands.

E-mail: ssiniscalchi@irec.cat
This work has received funding from the European Union's Horizon 2020 research and innovation programme under the Marie Skłodowska-Curie grant agreement No 675318 (INCITE).

Abstract. Nowadays, wind power plants (WPPs) should be able to dynamically change their power output to meet the power demanded by the transmission system operators. When the wind power generation exceeds the power demand, the WPP works in de-loading operation keeping some power reserve to be delivered into the grid to balance the frequency drop. This paper proposes to cast a model predictive control strategy as a multi-objective optimization problem which regulates the power set-points among the turbines in order to track the power demand profile, to maximize the power reserve, as well as to minimize the power losses in the inter-arrays connecting the wind turbines within the wind farm collection grid. The performance of the proposed control approach was evaluated for a wind farm of 12 turbines using a wind farm simulator to model the dynamic behavior of the wake propagation through the wind farm.

1. Introduction

Wind energy has experienced a very significant growth over the last decades becoming the second largest form of power generation capacity in Europe, going from 12.8 GW of total net installed capacity in 2000 to 168.7 GW by the end of 2017 [1]. This increasingly penetration level of wind power into the electricity network is posing some technical challenges in terms of grid stability due to the massive presence of non-synchronous generators in the electrical power system. Nowadays, in some European countries (such as Ireland, Spain and Germany), Transmission System Operators (TSOs) require WPPs to provide grid stability. To reach this goal wind power systems must be provided with suitable control strategies to enhance ancillary services, such as voltage and frequency support. The latter requires to keep the system in balance after frequency fluctuations by reducing or releasing more active power to balance the power supplied with the electricity demand. Therefore, in order to enhance a proper frequency support, WPPs must track the power demand profile required by TSOs.

For certain periods, the grid requirements can be met by de-loading the WPP by keeping a certain power reserve, which can still be delivered into the grid for helping in primary frequency support [2]. During de-loading operations, the tracking power can be achieved by different power contributions from each turbine within a WPP. The common approach is to distribute the power proportionally to the available power of each turbine [3]. However, recent works have proposed to solve optimization problems to dynamically distribute active power while maintaining the desired power production in order to: minimize the mechanical loads experienced by the turbines [4–6], to maximize the kinetic energy to enhance inertial support [7] and to maximize the power reserve to improve primary frequency support [8, 9]. In most of this works, the power references that the wind farm controller sends to each turbine are used as control action, whilst other authors consider a different approach based on using the axial induction factor as a control reference for ensuring active power control [10, 11].

In this paper, a control strategy based on model predictive control (MPC) is proposed. Here, the wind farm central controller uses the measurements of available and generated power of the turbines to optimize the power contribution of each turbine using the power reference as control action. The optimal sequence of control actions is found by solving a multi-objective optimization problem such that the overall power generated by the WPP tracks the power desired by the TSO. In case of de-loading operation, the additional degree-of-freedom for regulating the power contributions at the wind turbine level is used to minimize the wind speed deficits behind the upstream turbines, due to the wake effect, as well as to minimize the power losses in the inter-arrays connecting the wind turbines within the wind farm collection grid. The proposed control approach is evaluated for a wind farm of 12 turbines using a wind farm simulator where the wind field is generated by using the dynamic wake meandering model [12].

The remainder of this paper is organized as follows. The wind farm model and the cable losses model are discussed in Section II. Section III presents the multi-objective optimization problem and the MPC strategy. In Section IV the results are discussed. Finally, Section V presents the main conclusions.

2. System model

2.1. Wind Farm model

The power generated by a wind turbine is equal to

$$P_{\mathrm{g},i} = \min\left(\frac{1}{2}\rho A_D\, C_{\mathrm{p},i} v_i^3, P_{\mathrm{av},i}\right) \qquad \text{with} \qquad P_{\mathrm{av},i} = \min\left(\frac{1}{2}\rho A_D\, C_{\mathrm{p,max}} v_i^3, P_{\mathrm{rated}}\right), \quad (1)$$

where $A_D = \frac{\pi}{4}D^2$ with D the rotor diameter, ρ is the air density, v_i denotes the wind speed faced by the turbine i, P_{rated} is the rated power limit, and $C_{\mathrm{p,max}}$ is the maximum value of the power coefficient $C_{\mathrm{p},i}$. Based on the actuator disk theory [13], the latter can be written as

$$C_{\mathrm{p},i} = 4a_i(1-a_i)^2 \qquad \text{and} \qquad C_{\mathrm{p,max}} = C_{\mathrm{p},i}(a_i = 1/3), \quad (2)$$

where a_i is the axial induction factor that estimates how much the incoming wind speed v_i is affected by the generation condition of the turbine i. The interaction between rotor and incoming wind perturbs the outflow field and generates the wake effect. Wake effects involve complex phenomena leading to highly complex models, there exist multiple wake models (such as [12,14]) with different levels of accuracy and computational efforts depending on the study to be addressed. In this work, suitable estimation of the wind deficit behind the upstream turbine is obtained by modeling the wake as a quasi-steady state model with a linear relation between the induction factor and the downstream inlet velocity [14], i.e.,

$$v_j = v_i(1 - 2a_i c_{ij}) \qquad \text{with} \qquad c_{ij} = (D/(D + 2\kappa(s_{ij})))^2, \quad (3)$$

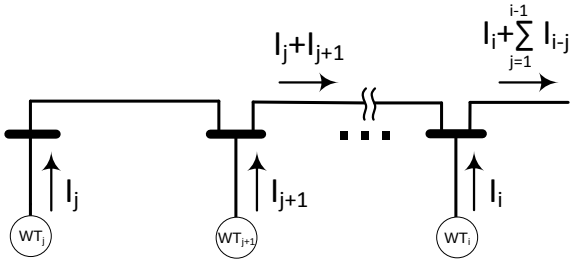

Figure 1. Electrical configuration of i turbines contected at the same feeder.

with $i \in \{1, \ldots, n_t - 1\}, j = i + 1$, κ the roughness coefficient, and c_{ij} a parameter depending on the separation between the turbines s_{ij}. Therefore, a variation of the induction factor can imply a change in the wind deficit and, thus in the available power for the single turbine $P_{\mathrm{a}v,i}$.

2.2. Cable losses model

Losses in power cables occur due to heat being dissipated from the interior of the cables towards the surroundings when the cables are energised and under load. Cable losses can be divided into conductor or ohmic losses due to the inner resistance of the cable, dielectric losses due to the charging current flowing through the capacitance created inside the isolation, and sheath and armour losses resulting from induced circulating currents within the conductor. For the sake of simplicity, this paper will only consider the ohmic losses, which are the main cause of losses in cables [15], specially in inter-array cables where cable lengths inter-connecting wind turbines within the collection grid are relatively short.

Ohmic or resistive losses in a cable i of length L_i can be calculated as

$$P_i^{\mathrm{loss}} = R_i I_i^2, \text{ with } \qquad R_i = r_i L_i, \tag{4}$$

where R_i, r_i are respectively the cable resistance and the resistance per unit of cable length and I_i is the current that flows through the cable.

For this study, it is assumed that reactive power flowing among wind turbines is small (i.e., the power factor is close to one) and the voltage magnitudes in each bus within the collection grid are very close to the nominal value, so that voltage drops are negligible [16]. Thus, the current flowing for each inter-array cable i can be estimated as

$$I_i = \frac{P_i}{V_{\mathrm{n}}}, \tag{5}$$

where P_i is the active power flowing through the cable i and V_n the voltage nominal value.

Assuming a radial electrical configuration within the wind farm (see Figure 1), and replacing expression (5) in (4), the power losses in a certain cable i belongs to a feeder k connecting several turbines is

$$P_{k,i}^{\mathrm{loss}} = \frac{R_{k,i}}{V_{\mathrm{n}}^2}(P_{\mathrm{g},i} + \sum_{j=1, i\geq 2}^{i-1} P_{\mathrm{g},j})^2, \qquad \forall i \geqslant 2, \tag{6}$$

where $P_{\mathrm{g},i}$ is the power generated by turbine i connected to the cable i defined in (1) and $P_{\mathrm{g},j}$ refers to the power generated by the turbine j located before the turbine i and connected at the same feeder k. Hence, the total power losses in a wind farm of n_t turbines with l feeders and N turbines for each feeder is denoted by

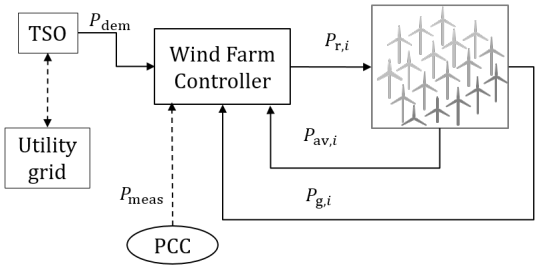

Figure 2. Closed-loop control scheme.

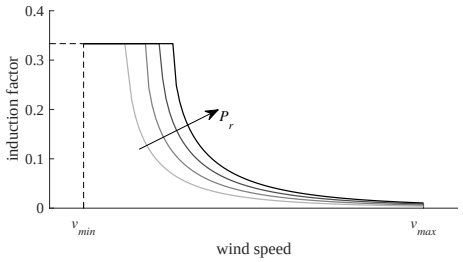

Figure 3. Induction factor a – wind speed v characteristic for several power set-points P_{r}. The black line corresponds to the nominal case ($P_{\text{r}} = P_{\text{rated}}$).

$$P_{\text{tot}}^{\text{loss}} = \frac{1}{V_{\text{n}}^2}\mathbf{R}\,(\mathbf{K}\,\mathbf{P_g^2}), \tag{7}$$

where

$$\mathbf{R} = \begin{bmatrix} R_{1,1} & \cdots & R_{1,N} \\ \vdots & \ddots & \vdots \\ R_{l,1} & \cdots & R_{l,N} \end{bmatrix} \in \mathbb{R}^{l\times N}, \qquad \mathbf{P}_g = [P_{g,1},\ldots,P_{g,n_t}]^T \in \mathbb{R}^{n_t} \tag{8}$$

$$\mathbf{K} = diag[K_1,\ldots,K_l] \in \mathbb{R}^{(l\times N)\times n_t} \qquad K_i = \begin{bmatrix} 1 & & \\ \vdots & \ddots & \\ 1 & \cdots & 1 \end{bmatrix}. \tag{9}$$

Here $\mathbf{R}$ denotes the resistence matrix, $\mathbf{P}_g$ the vector of generated powers, and $\mathbf{K}$ a block diagonal matrix, for which each element is equal to the matrix K_i.

3. Control Strategy

In Figure 2, the wind farm control scheme is shown. The wind farm controller acts as a single centralized unit, which has as inputs the power demanded by the TSO P_{dem}, the measurements P_{meas} from the point of common coupling (PCC), the power generated $P_{g,i}$ and available $P_{av,i}$ from the wind turbines, while as outputs the power references for each turbine namely $P_{r,i}$. The latter are sought by solving a multi-objective optimization problem stated to regulate the total power delivered by the wind farm at the PCC.

3.1. Problem Statement

The solution of the optimization problem consists in finding the sequence of the optimal power reference $\mathbf{P}_r^* = [P_{r,1}^*,\ldots,P_{r,n_t}^*]^T$ to be addressed at the wind turbines such that the following objectives are minimized:

O1) *Tracking error*: minimize the difference between power demand required by the TSO and total mechanical power generated by the wind turbines. This objective can be denoted as

$$J_1 = P_{\text{dem}} - \sum_{i=1}^{n_t} P_{\text{g}i} \tag{10}$$

O2) *Peaks on power generation*: minimize the variation over the control inputs to avoid peaks in the power output, i.e. power generated, avoiding possible damage due to quick variations on the mechanical loads affecting the turbines. This objective is defined as

$$J_2 = \Delta \mathbf{P}_{\mathrm{r}}. \tag{11}$$

O3) *Wake effect*: minimize the wind deficits, i.e. maximize the power available.
In order to ensure this objective the sequence of $P_{\mathrm{r},i}$ should be found by properly setting the axial induction factors a_i that minimize the wind deficits. As can be seen in Figure 3, there exists a one-to-one relation between $P_{\mathrm{r},i}$ and a_i. In order to maximize the available power, the most down-stream wind turbines should contribute more to the total generated power. There are several proposals to do this, see for example [9]. Here, a simple weighted sum is used in order to simplify the entire optimization problem. The weights are selected according to the wind farm layout and predominant wind speed directions. That is,

$$J_3 = \sum_{i=1}^{n_t} \omega_i P_{\mathrm{g},i}. \tag{12}$$

Assuming the set of turbine indices to be $\aleph = \{i : 1 \leq i \leq n_t \text{ with } v_i \geq v_j, \text{ for } i < j\}$, then the weights $\omega_i \in [0, 1]$ must satisfy $\omega_1 \geq \omega_2 \geq \cdots \geq \omega_{n_t}$. Notice that the set $\aleph$ is sorted to the dominant free-stream wind speed direction, such that $i = 1$ indicates the turbine facing the free-stream wind speed while $i = n_t$ is the turbine most affected by the wakes. Hence, the same weights correspond to the turbines facing the same wind conditions.

O4) *Power losses*: minimize the electrical power losses. Hence, according to (7) the objective is denoted by

$$J_4 = P_{\mathrm{tot}}^{\mathrm{loss}}. \tag{13}$$

The aforementioned objectives are prioritized by setting the vector of weights $\mathbf{w} \in \mathbb{R}^4_{\geq 0}$ in (15). The primary objective of the wind farm controller is to ensure the power required by the TSO and to guarantee the safety of the wind turbines, thus the highest priority is given to the first and second objectives. However, in case of de-loading operations the previous goal can be achieved regulating the power contribution of the turbines in different ways. To this end, the latter two objectives are properly prioritized to find an optimal power distribution for each turbine ensuring both minimization of power losses and maximization of power reserve.

3.2. Multi-objective predictive controller

In this section an MPC strategy is proposed to solve the multi-objective optimization problem. The wind turbine system has been shown to be properly modelled as a first-order system [8], hence the dynamical model to be controlled is given by

$$\mathbf{x}_{k+1} = \mathbf{A}_d \mathbf{x}_k + \mathbf{B}_{1d} \mathbf{u}_k + \mathbf{B}_{2d} P_{\mathrm{dem}}, \tag{14}$$

where $k \in \mathbb{Z}_{\geq 0}$ denotes the discrete-time step, $\mathbf{x}_k = [\mathbf{P}_{\mathrm{g},k}^T, \xi]^T \in \mathbb{R}^{n_x}$ is the vector of system states, $\mathbf{P}_{\mathrm{g},k} \in \mathbb{R}^{n_t}$ is the vector of generated powers, ξ is an integral action to ensure a zero steady-state tracking error and $\mathbf{u}_k \in \mathbb{R}^{n_u}$ denotes the vector of control inputs corresponding to the vector of manipulated power references $\mathbf{u} = [P_{r,1}, \ldots, P_{r,n_t}] \in \mathbb{R}^u$. Moreover, the formulation of the discrete-time matrices $\mathbf{A}_d$, $\mathbf{B}_{1d}$ and $\mathbf{B}_{2d}$ depending on the ime constant used to model the wind turbine system is elaborated in [8].

In order to design the MPC strategy for the considered system, let $\hat{\mathbf{u}}(k) \triangleq \{\mathbf{P}_r(k|k), \ldots, \mathbf{P}_r(k + H_p - 1|k)\}$ be a set of feasible control inputs within a pre-established prediction horizon $H_p \in \mathbb{Z}_{>0}$ that is constrained to ensure desired operational limits. Consider

that the system (14) is controlled using the multi-objective optimization problem with $m = 4$ control objectives. Thus, the optimization problem behind the MPC controller is stated as follows:

$$\begin{aligned} &\underset{\hat{\mathbf{u}}(k)}{\text{minimize}} \quad \sum_{j=1}^{m} w_j J_j(\mathbf{x}_k, \hat{\mathbf{u}}_k) \\ &\text{subject to} \\ &\quad \mathbf{x}_{(k+j+1|k)} = \mathbf{A}_d \mathbf{x}_{(k+j|k)} + \mathbf{B}_d \mathbf{u}_{(k+j|k)} + \mathbf{B}_l P_{dem} \quad j \in [0, H_p - 1] \cap \mathbb{Z}_{\geq 0} \\ &\quad P_{\min} \leq \mathbf{u}_{(k+j|k)} \leq \mathbf{P}_{\text{av}}(k) \end{aligned} \tag{15}$$

being $P_{\min}$ and $\mathbf{P}_{\text{av}}$ respectively the minimum and maximum power limits. Note that the former is included to avoid the shutdown of the turbines. The solution of the optimization problem finds the sequence of the optimal power set-point $\mathbf{u}^* = [P^*_{r,1}, \ldots, P^*_{r,n_t}]$ such that the objectives aforementioned are minimized.

Taking into account the parameters used to define the dynamical wind turbine model, the cost functions from J_1 to J_4 should be rewritten as,

O1) $J_1 = (Q\mathbf{x}_k)'(Q\mathbf{x}_k)$, with $Q = [0, \ldots, 0, 1] \in \mathbf{R}^{n_x}$.
O2) $J_2 = (S\Delta\mathbf{u}_k)'(S\Delta\mathbf{u}_k)$, with $\Delta\mathbf{u}_k = \mathbf{u}_k - \mathbf{u}_{k-1}$ and $S = \mathbf{I}_{n_t}$.
O3) $J_3 = \mathbf{1}_{n_t}(\Omega\mathbf{x}_k)$, with $\Omega = blkdiag[\omega_1, \ldots, \omega_{n_t}] \in \mathbb{R}^{n_t}$.
O4) $J_4 = P^{loss}_{tot,k}$.

Notice that the total power loss is neglected in the evaluation of f_1, being at most fourth order of magnitude lower than the power demand. Moreover, such an assumption allows to guarantee the linearity of the optimization problem.

4. Case Study

A wind farm layout of 12 wind turbines laid in 3 rows and 4 columns is considered to test the proposed control strategy. The 5-MW NREL benchmark turbines are used and spaced $5D$ (i.e. 630 m) in both the x and y direction. The inter-array cables considered for this study are 3-phase XLPE-Cu, operating at 33 kV and are connected as shown in Figure 4. In Table 1 the cable parameters are presented. The AEOLUS SimWindFarm (SWF) Simulink toolbox [17] has been used for simulating the wind speed at wind farm grid points in two dimensions. Wake effects within the wind farm is modeled according to the dynamic wake meandering model [12] for given ambient turbulent intensity and wind speed direction. In order to have a clearer view of the power available and power losses changes prodecued applying the proposed strategy, a laminar flow is modeled using a grid size of 2500×2500 m^2 and the points are spaced 15 m. Figure 5 shows the steady-state wind field through the wind farm with wind direction of 0 degrees.

The dynamic model (14) has been discretized using a sampling time of 0.01 s and a prediction horizon $H_p = 4$ s is selected, small enough to regulate the power generation within milliseconds. Wind turbine has been modeled as a first order model with a time constant (τ) set at 0.08 s. In order to ensure the priority of the multi-objectives functions as presented in Section 3, the vector of weights in (15) is set equal to $\mathbf{w} = [10, 4.5, 10^4, 1.26e^6]$ such that similar relevance between the quadratic and linear cost functions is obtained.

In order to see the benefits of improving power available for enhancing frequency support, the results are referred to the power reserve of the wind farm. This is the active power that can be delivered into the grid to supply the imbalance after a frequency event defined as

$$P_{\text{res}} = \sum_{i=1}^{n_t} (P_{\text{av},i} - P_{\text{dem}}). \tag{16}$$

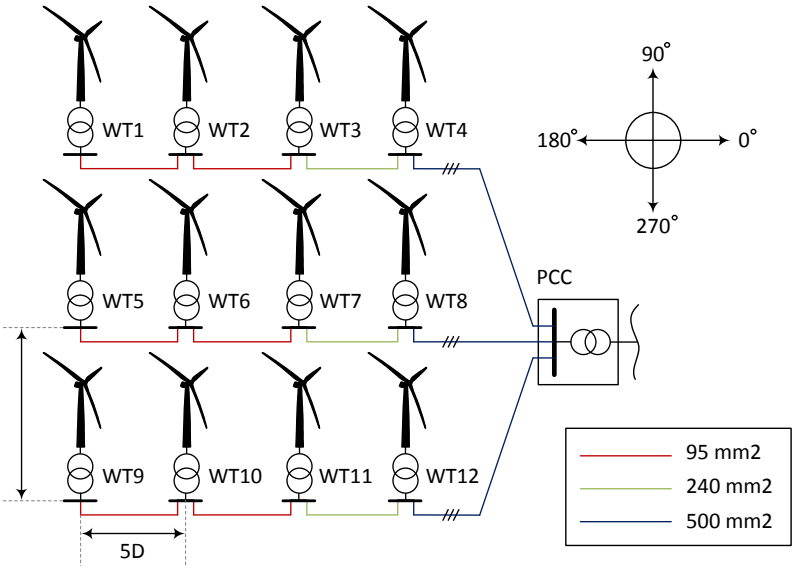

Figure 4. Wind farm layout.

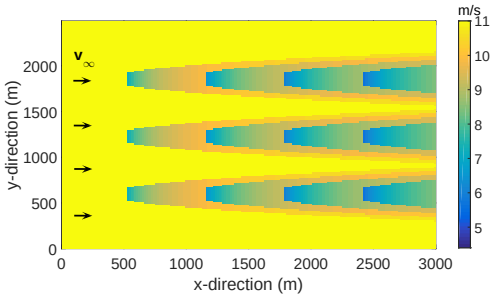

Figure 5. Wind flow field simulated with SWF.

Cross section [mm^2]	Resistance [Ω/km]
95	0.248
240	0.098
500	0.0456

Figure 6. Cable parameters [18].

Two scenarios are simulated as follows. The first scenario analyzes the system response of the wind farm controller when the power required by TSO changes dynamically during the simulation time. The second scenario shows the effects on the power reserve and the power losses when the proposed multi-objective optimization problem is solved by the wind farm controller. In both cases, the free-stream wind speed is equal to $v_\infty = 11$ m/s.

4.1. Scenario 1: Power tracking

Figure 7 shows the power response of the system for a wind speed coming from 0 degrees. The wind farm works in derated operation, hence the available power (blue line) is higher than the power demand profile (red line). The proposed control strategy ensures that the total power generated by the farm (grey-dashed line) tracks the fast variations of the power demand ensuring that the tracking error is kept lower than 0.12% of the average power demand.

In order to see how the controller optimizes the power set-points among the turbines, Figure 8 shows the available, generated and reference powers for each turbine. According to the cost functions J_3 and J_4 in (15) the power set-points for each turbine are found to improve the overall power reserve while decreasing the electrical cable losses. The latter is reduced by minimizing the powers generated by the turbines furthest from the PCC, see Figure 4. Meanwhile the power

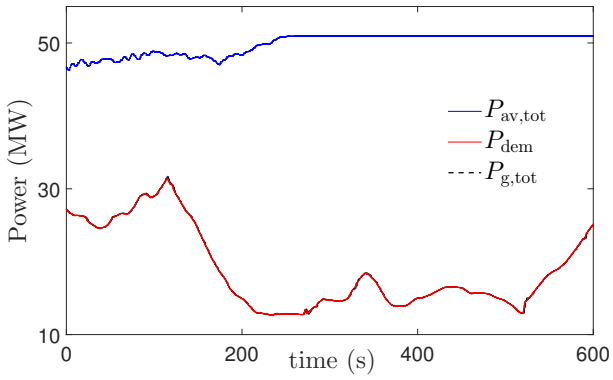

Figure 7. Scenario 1: Available $P_{\text{av,tot}}$, demanded P_{dem}, and generated $P_{\text{g,tot}}$ wind farm powers.

reserve is improved reducing the wake effect throught the wind farm, then improving the overall power available of the farm. As stated in Section 3, in order to reduce the wake effect the power references are set such that the highest power contribution is required to the most downstream turbines while the power generation of the other turbines is reduced until to have the minimum power generated from the most downstream turbines. Until time $0 \leq t \leq 150$ s in order to track the power demand the power generated by the wind turbines (3-7-11-4-8-12 WTs) produce exactly the available power, while the upstream turbines (1-5-9 WTs) generate the minimum power 1 MW, which avoids the shutdown. At time $t \geq 150$ s, when the power demand decreases, only the most downstream turbines (4-8-12 WTs) are required to produce more power. The effect of the aforementioned optimal power distribution in overall power reserve and electrical power losses are shown in Figure 9. Here, two cases are compared: Case 1 (grey line) is obtained when the MPC is stated to minimize only the first two objectives J_1 and J_2, that is only tracking is acheived. Case 2 (green line) all the full multi-objective optimization problem in (15) is solved. The power reserve improves while the power losses decrease.

4.2. Scenario 2: Power regulation for different wind directions

For a more comprehensive evaluation of the proposed control strategy towards power reserve maximization and power losses minimization, the system model is simulated for $t < t_1$ to ensure only tracking. Therefore, the cost function in (15) includes only the first and second objective functions (f_1 and f_2. Then, for $t > t_1$ the complete multi-objective problem is solved. In this scenario, in order to have a clearer evaluation of the power distribution, the power demand is kept constant at $P_{\text{dem}} = 30$ MW. Figure 10 shows the power set-points (dashed grey line), the power generation (red line) and the power available (blue line) for each wind turbine. Initially, the tracking is ensured by requiring the same contribution for each turbine, which is equal to 2.5 MW. Then, for $t > t_1$ the power distribution changes. The controller seeks to find the optimal power references for the turbines that ensure minimization of both wake effects and power losses. Here, the power generation of the first column is reduced to 2.8 MW, while the powers produced by the third and the last columns are respectively increased to 3 MW and to the maximum available power. Meanwhile, the generation for the second column is kept constant at 2.5 MW. As discussed in Section 2, the reduction of the power contribution of the turbines in the first column increases their induction factors such that also the wind speed deficits in (3) are decreased and the powers available improved. However, the effects in the variations of the power set-points can be seen only after certain periods denoted by k_i, which depend on the travel time required by the wakes to cross the wind farm. In Figure 11 are shown the power

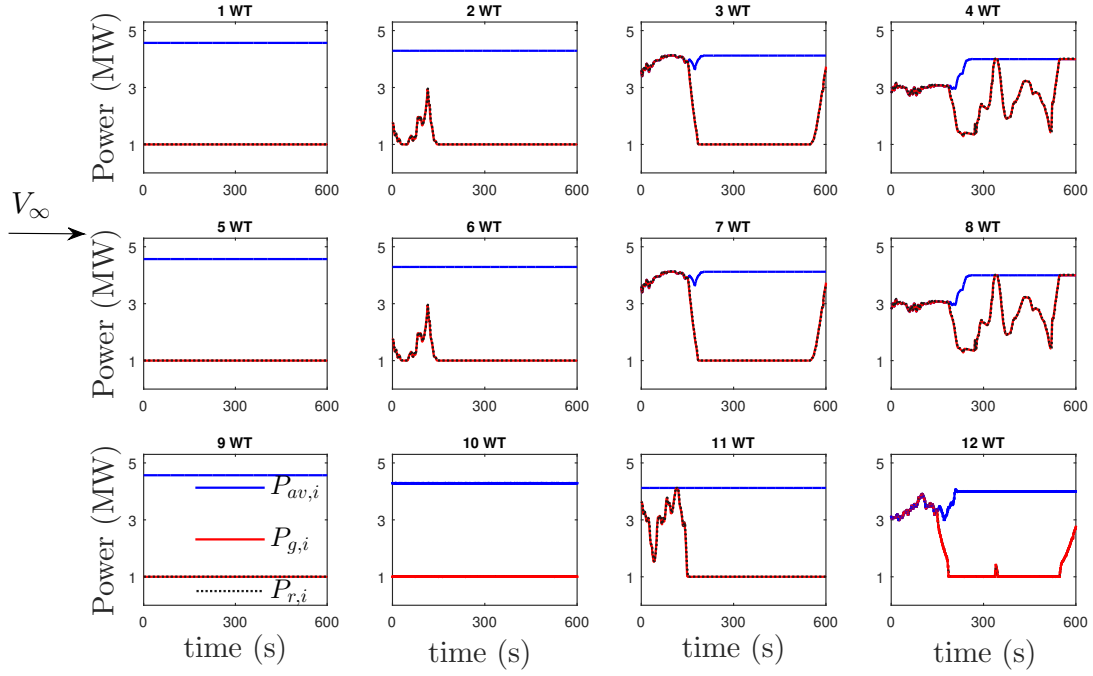

Figure 8. Scenario 1: Power generated $P_{g,i}$, available $P_{av,i}$, and power set-points required by the controller $P_{r,i}$)

.

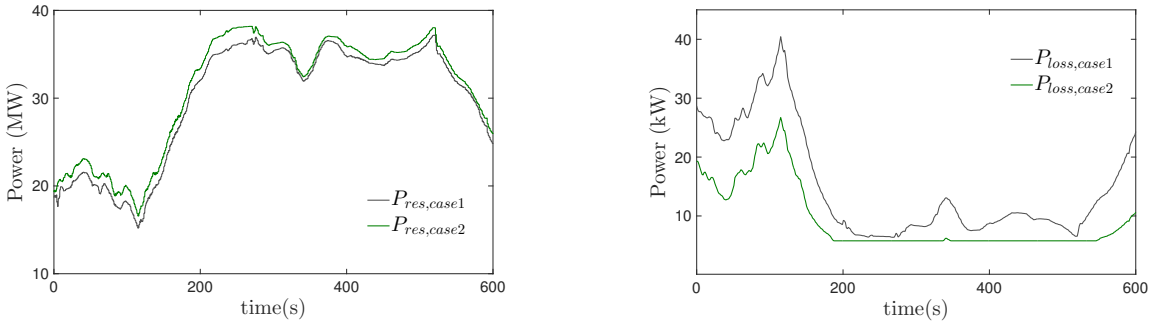

Figure 9. Scenario 1: Power reserve and power losses profiles.

reserve and electrical power losses for several wind directions.

The minimization of power losses is obtained for each direction by reducing the power generation of the turbines closer to the PCC. Meanwhile, the decreasing of the wind deficits is achieved by generating more power with the downstream turbines, which change according to the direction of the wind. Therefore, the best balance between the two objectives is obtained for a wind direction of 0 degrees.

5. Conclusions

A multi-objective optimization problem for wind farms that is solved with the predictive control model technique has been presented in this work. Typically, to enhance frequency support wind farms should track the fast variations of the power demand profile required by the TSO and

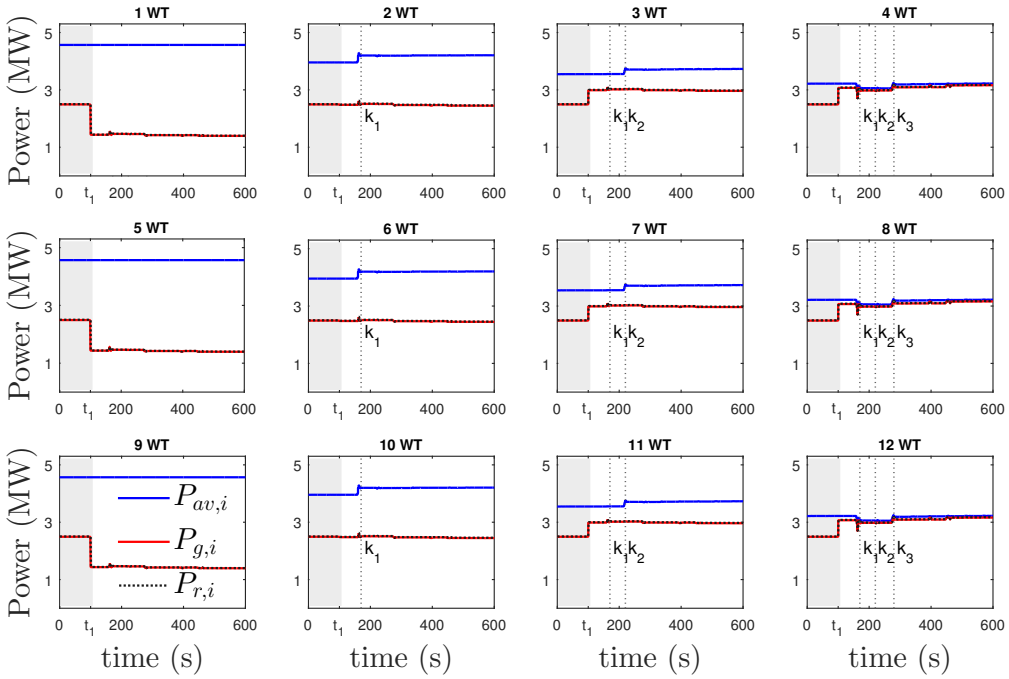

Figure 10. Scenario 2: Power generated $P_{\mathrm{g},i}$, available $P_{\mathrm{av},i}$ and power set-points required by the controller $P_{\mathrm{r},i}$).

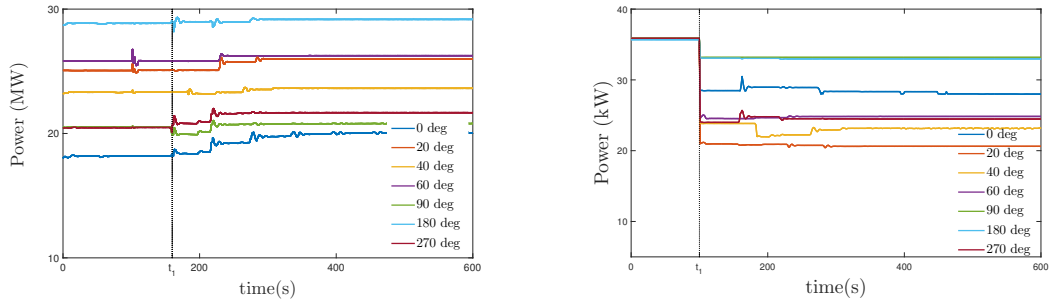

Figure 11. Scenario 2: Power reserve and power loss for several wind direction.

deliver some additional active power to reduce the power imbalances due to a frequency event. The proposed control strategy ensures a proper tracking of the power demand while improving the overall capacity reserve and reducing the active power losses in the electrical inter-array connecting the turbines. The strategy has been tested for a wind farm of 12 WTs under several wind directions. The results have shown that the tracking is well ensured while the power reserve increases for all the simulation cases, in particular the highest improvement is achieved when the turbines are extremely affected by the wakes (i.e. at 0 degrees). Finally, also the overall power losses through the cables are reduced for all the investigated cases, in particular the highest reduction has been shown when the upstream turbines coincide with the turbines closest to the PCC.

References

[1] WindEurope. Wind energy in europe, scenarios for 2030, Sep. 2017.

[2] EWEA. Balacing responsability and costs of wind power plants, 2015.

[3] Anca D Hansen, Poul Sørensen, Florin Iov, and Frede Blaabjerg. Centralised power control of wind farm with doubly fed induction generators. *Renewable Energy*, 31(7):935–951, 2006.

[4] Baohua Zhang, Mohsen Soltani, Weihao Hu, Peng Hou, Qi Huang, and Zhe Chen. Optimized power dispatch in wind farms for power maximizing considering fatigue loads. *IEEE Transactions on Sustainable Energy*, 2017.

[5] Paul A Fleming. Active power control of waked wind farms: Preprint. Technical report, National Renewable Energy Lab.(NREL), Golden, CO (United States), 2017.

[6] Jan-Willem van Wingerden, Lucy Pao, Jacob Aho, and Paul Fleming. Active power control of waked wind farms. *IFAC-PapersOnLine*, 50(1):4484–4491, 2017.

[7] Antonio De Paola, David Angeli, and Goran Strbac. Scheduling of wind farms for optimal frequency response and energy recovery. *IEEE Transactions on Control Systems Technology*, 24(5):1764–1778, 2016.

[8] Sara Siniscalchi Minna, Fernando Bianchi, and Carlos Ocampo Martinez. Predictve control of wind farms based on lexicographic minimizers for power reserve maximization. In *Proc. of American Control Conference (ACC)*. IEEE, 2018.

[9] Sara Siniscalchi Minna, Fernando Bianchi, Mikel De Prada Gil, and Carlos Ocampo Martinez. A wind farm control strategy for power reserve maximization. *Renewable Energy*, under review.

[10] Sjoerd Boersma, Bart Doekemeijer, Mehdi Vali, Johan Meyers, and Jan-Willem van Wingerden. A control-oriented dynamic wind farm model: Wfsim. *Wind Energy Science*, 3(1):75–95, 2018.

[11] PMO Gebraad and JW Wingerden. Maximum power-point tracking control for wind farms. *Wind Energy*, 18(3):429–447, 2015.

[12] Gunner C Larsen, Helge Aa Madsen, Kenneth Thomsen, and Torben J Larsen. Wake meandering: a pragmatic approach. *Wind energy*, 11(4):377–395, 2008.

[13] James F Manwell, Jon G McGowan, and Anthony L Rogers. *Wind energy explained: theory, design and application*. John Wiley & Sons, 2010.

[14] N. O. Jensen. A note on wind generator interaction. Technical report, Roskilde, Denmark, 1983.

[15] M. Fischetti and D. Pisinger. Optimizing wind farm cable routing considering power losses. *European Journal of Operational Research*, 2017.

[16] A. Ameri, A. Ounissa, C. Nichita, and A. Djamal. Power loss analysis for wind power grid integration based on weibull distribution. *Energies*, 10(4):1–16, 2017.

[17] J. Grunnet, M. Soltani, T. Knudsen, M. Kragelund, and T. Bak. Aeolus toolbox for dynamics wind farm model, simulation and control. In *The European Wind Energy Conference & Exhibition, EWEC*, 2010.

[18] HAVELLS. https://www.havells.com/content/dam/havells/brouchers/industrial2009.